

TRANSVERSE IMPEDANCE OF ELLIPTICAL CROSS-SECTION TAPERS*

Boris Podobedov[#], Samuel Krinsky, BNL/NSLS, Upton, New York

Abstract

We investigate the transverse impedance of elliptical cross-section tapers. Analytical estimates for the dipolar and quadrupolar components of the impedance at low frequency are obtained by extending a perturbation approach introduced by Stupakov. The perturbation theory results are compared to EM code GdfidL and are found to be in excellent agreement.

INTRODUCTION

An important issue in the design of modern synchrotron light sources is the determination of the transverse impedance of vacuum chambers for small-gap undulators which have tapers going from one cross-section to another in a given length. Similar problems occur in the collimator design for high energy physics machines, as well as designs of other common transitions. In typical cases of interest, the tapering is sufficiently gradual to be effective, the chamber height changes by a substantial factor, and the horizontal-to-vertical aspect ratio is large.

Yokoya has derived the low frequency transverse impedance of an axially symmetric tapered transition [1]. Later, Stupakov [2] used first-order perturbation theory to provide a new derivation of Yokoya's result at zero frequency ($k = 0$), based on the solution of electrostatic and magnetostatic problems. Using this technique, Stupakov [3] also determined the vertical impedance of a flat rectangular chamber of constant half-width w and varying half-height $h(z) \ll w$, resulting in impedance much larger than that for a round chamber of the same vertical profile.

Recently, we have used Stupakov's approach to calculate the horizontal and vertical impedances at $k = 0$ of an elliptical taper [4]. In the present paper, we extend our earlier work by determining the quadrupolar components [5] of the impedance. These components, only present in axially asymmetric structures, are due to forces proportional to the displacement of the trailing charge, unlike the dipolar impedance which depends on the displacement of the leading charge. The quadrupolar components are important as they contribute to incoherent tune shift, and typically improve beam stability through Landau damping. While quadrupolar impedances have been analyzed for the case of resistive wall [6] to our knowledge there are no previous analytical results determining the quadrupolar impedance arising from geometry variation of the vacuum chamber.

Since our previous publication [4], we have: improved our EM code calculations by switching to convex structures; extended our treatment to higher perturbation theory orders to clarify the applicability range; and determined the quadrupolar impedance.

*Work supported by DOE contract number DE-AC02-98CH10886.

[#]boris@bnl.gov

ANALYTICAL RESULTS

Stupakov's [2] method involves solving inhomogeneous two-dimensional Poisson equations. Matching boundary conditions for a translation invariant (uniform) elliptical cross-section is most easily done using elliptic cylindrical coordinates (μ, θ, z) . The contour surfaces of constant μ are confocal elliptical cylinders, while those of constant θ are confocal hyperbolic cylinders. The confocal cylinder $\mu = \rho$ forms the inner beam pipe boundary, while the z -axis is directed along the chamber axis. The relationship between Cartesian and elliptic coordinates is given by

$$\begin{aligned} x &= A \cosh \mu \cos \theta \\ y &= A \sinh \mu \sin \theta \\ z &= z \end{aligned} \tag{1}$$

where $2A$ is the distance between the foci. The major and minor semi-axes of the elliptical cross-section are $a = A \cosh \rho$ and $b = A \sinh \rho$, and its eccentricity is given by $e = \sqrt{1 - b^2/a^2} = 1/\cosh \rho$. The limiting case of a circular cross-section of radius r is given by $A = 2r \exp(-\rho)$, with $\rho \rightarrow \infty$. The limit of $\rho \rightarrow 0$, approximates a flat pipe $2h = 2A\rho$ high by $2w = 2A$ wide.

In the case when the elliptical cross-section varies with z , it is generally not possible to introduce an orthogonal coordinate system that matches the cross-section at each value of z . However, when the variation maintains a confocal structure, we can use the elliptic cylindrical coordinates introduced above, allowing ρ to have a z -dependence. The horizontal-to-vertical aspect ratio is given by $a(z)/b(z) = 1/\tanh \rho(z)$ and the constant A is determined by $A^2 = a(z)^2 - b(z)^2$. The requirement for confocal variation allows arbitrary variation in one plane, e.g. arbitrary beam pipe half-height $b(z)$. The variation in the other plane is then fixed as soon as a is specified at any single value of z .

Consider the wakefield produced by a drive charge with transverse coordinates (x_d, y_d) to be sampled by a test charge at transverse coordinates (x_t, y_t) . To lowest order in the transverse coordinates this wakefield can be decomposed into the dipolar and quadrupolar parts in each plane [5]. Similarly, in the frequency domain the horizontal and vertical impedances are given by

$$\begin{aligned} Z_x(x_d, y_d; x_t, y_t; k) &\cong Z_{D_x}(k)x_d + Z_Q(k)x_t \\ Z_y(x_d, y_d; x_t, y_t; k) &\cong Z_{D_y}(k)y_d - Z_Q(k)y_t \end{aligned} \tag{2}$$

Within first-order perturbation theory [4], we find

$$Z_{D_x} = - \sum_{n=1,3,\dots} \int_{-\infty}^{\infty} dz f_n(z) \left[\frac{n}{\cosh^2 n \rho} + \frac{n+2}{\cosh^2(n+2)\rho} \right]^2 \quad (3a)$$

$$Z_{D_y} = - \sum_{n=1,3,\dots} \int_{-\infty}^{\infty} dz f_n(z) \left[\frac{n}{\sinh^2 n \rho} + \frac{n+2}{\sinh^2(n+2)\rho} \right]^2 \quad (3b)$$

$$Z_Q = \sum_{n=0,2,\dots} \int_{-\infty}^{\infty} dz f_n(z) \left[\frac{1}{\cosh^2 n \rho} + \frac{1}{\cosh^2(n+2)\rho} \right] \times \left[\frac{n^2}{\cosh^2 n \rho} + \frac{(n+2)^2}{\cosh^2(n+2)\rho} \right] \quad (3c)$$

where

$$f_n(z) = \frac{iZ_0}{4\pi} \frac{\rho'(z)^2}{2(n+1)} \sinh 2(n+1)\rho, \quad (4)$$

Z_0 is the free space impedance and $k = 0$ is assumed.

In the limit of a round pipe ($\rho \rightarrow \infty$), the dipolar impedances reduce to the result originally found by Yokoya [1],

$$Z_{D_x} = Z_{D_y} \equiv Z_{round} \equiv -\frac{iZ_0}{2\pi} \int_{-\infty}^{\infty} dz \frac{\rho'(z)^2}{\rho(z)^2}, \quad (5)$$

and the quadrupolar impedance Z_Q vanishes.

In the limit of a flat pipe ($\rho \rightarrow 0$), we derive

$$Z_{D_x} \equiv -\frac{iZ_0}{4\pi} \int_{-\infty}^{\infty} dz \frac{\rho'(z)^2}{\rho(z)^2} \quad (6a)$$

$$Z_{D_y} \equiv -\frac{iZ_0 \pi}{16} \int_{-\infty}^{\infty} dz \frac{\rho'(z)^2}{\rho(z)^3} \quad (6b)$$

$$Z_Q \equiv \frac{iZ_0}{4\pi} \int_{-\infty}^{\infty} dz \frac{\rho'(z)^2}{\rho(z)^2} \quad (6c)$$

Note that in this limit, the horizontal dipolar and quadrupolar impedances have equal magnitude $Z_{round} / 2$ but opposite signs. From Eq. (2), we see that this implies that a trailing bunch displaced horizontally by the same amount as the drive bunch does not experience any force in a flat chamber. Eq. (6b) for Z_{D_y} is similar to that of a flat rectangular pipe result of [3] but is lower by $\pi/8$.

Impedance expressions presented above are the results for the first order perturbation theory, the lowest one to give non-vanishing values. To find out the range of validity of these results we have extended our treatment to higher orders. For arbitrary ellipticity, even the second order impedance formulas are very long. In the limiting case ($\rho \rightarrow 0$) of a smooth flat chamber, we found that the horizontal and quadrupolar impedance second order corrections are small for taper length ℓ , if the average chamber height satisfies $h_{av}^2 / \ell^2 \ll 1$. In contrast, in order to assure that second order terms for the vertical dipolar impedance are small, it is additionally required that the chamber width satisfies $w_{av}^2 / \ell^2 \ll 1$. Therefore, the perturbation theory breaks down when the taper width is comparable to or larger than its length.

In the case of a round taper, we carried out a more detailed study of the contributions of the higher-order terms in the perturbation theory [7].

COMPARISON WITH GDFIDL

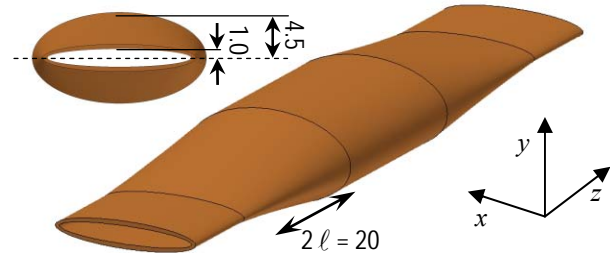


Figure 1: Geometry with principal dimensions in cm.

We now discuss calculations performed using code GdfidL [8] for the geometry of Fig. 1, consisting of a uniform pipe with elliptical cross-section linearly tapered to another uniform elliptical pipe with a larger cross-section confocal to the first pipe; the structure is then continued mirror symmetrically with respect to the middle of the center pipe. The center pipe is chosen long enough that we are in the regime of two non-interacting tapers.

The vertical and axial dimensions are fixed for all calculations. Both the outer and the inner pipes are then varied from round to approximately flat maintaining the confocal condition. In each case, we separately calculate the horizontal and vertical dipolar wake-potentials by displacing the 1 cm rms long drive bunch in the appropriate plane, or running it on axis for the quadrupolar case. We take advantage of the symmetry planes and perform the calculations for a quarter structure, $x > 0, y > 0$, enforcing electric boundary condition in the $y=0$ ($x=0$) plane and magnetic boundary condition in $x=0$ ($y=0$) plane when calculating vertical (horizontal) dipolar wake-potentials. Both boundaries were set to magnetic for quadrupolar wake calculations. To get the zero frequency impedance we integrated the wake-potential over 2 m distance behind the drive bunch and normalized the result to the displacement of the driving (trailing) particle for the dipolar (quadrupolar) case.

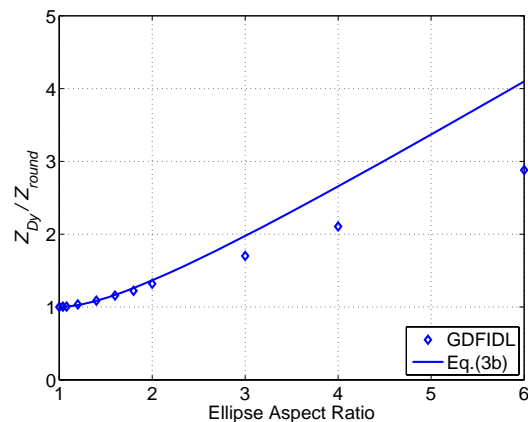


Figure 2: Dipolar vertical impedance.

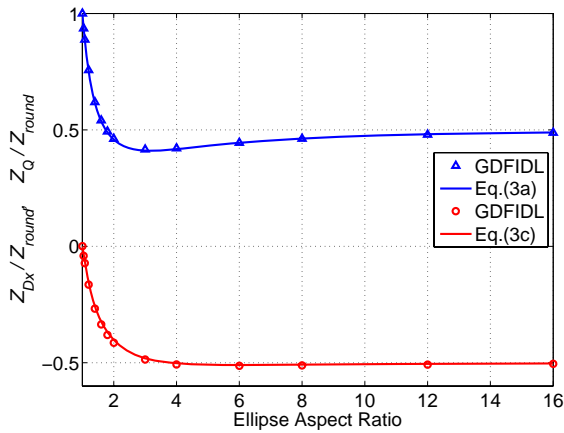


Figure 3: Dipolar horizontal and quadrupolar impedances.

Transverse impedances found in this manner are shown in Figs. 2-3. They are normalized by the GdfidL values of dipolar impedance of axially symmetric pipe with the same vertical profile. For the 0.4 mm step size used the GdfidL value for the round pipe ($\sim 1.8 \text{ k}\Omega/\text{m}$) is quite close to $1.7 \text{ k}\Omega/\text{m}$ that follows from Eq. (5). We plot this impedance vs. the ellipse aspect ratio always taken at the smallest cross-section (where the chamber is the most flat). GdfidL calculations of Z_Q were done twice, with either vertical or horizontal trailing charge displacement; the results came out essentially the same.

Also plotted are the first order perturbation theory results from Eqs. (3a-c). For vertical impedance (Fig. 2) there is a good agreement with GdfidL up to aspect ratio of ~ 3 where $w_{av}^2/\ell^2 \approx 0.17$ and higher order terms become important. Horizontal and quadrupolar impedances (Fig. 3) exhibit good agreement for all aspect ratios, consistently with the gradually tapered structure in hand ($h_{av}^2/\ell^2 \approx 0.076$). Interestingly, both Z_{Dx} and Z_Q achieve their “flat limit” at rather low aspect ratio of ~ 2 . Similar behaviour was found for resistive wall impedance in uniform pipes with elliptical cross-section (i.e. [6]).

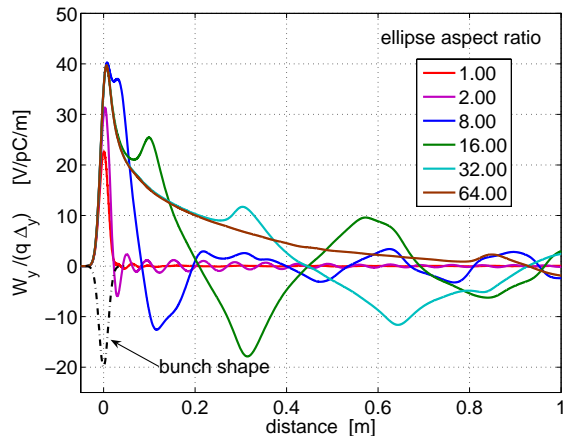


Figure 4: Dipolar vertical wake potentials.

Additional insights come directly from the wake-potentials calculated by GdfidL. For the horizontal and

quadrupolar cases these are basically proportional to the bunch shape, implying that impedance is essentially a constant inductance equal to that plotted in Fig. 3. For the vertical the situation is different as indicated in Fig. 4 where we present wake-potentials from GdfidL for aspect ratios up to 64. Past aspect ratio of ~ 2 the wake potential starts widening much beyond the drive bunch shape, while its peak height saturates. As a result Z_{Dy} grows to substantial values ($\sim 10 Z_{round}$ for our geometry) before saturation, while the kick factor saturates at a much more modest level of \sim twice the round pipe value. This means that the vertical taper impedance implications for single bunch dynamics are far less severe than what would follow from Eq. (6b) or the result of [3].

CONCLUSION

We derived analytical expressions for the low frequency transverse impedance of slow tapered structures with elliptical cross-section. Our results show excellent agreement with GdfidL. Apart from slow tapering ($h_{av}^2/\ell^2 \ll 1$), an extra condition ($w_{av}^2/\ell^2 \ll 1$) is necessary for the validity of the vertical dipolar impedance expression obtained.

In the limit of flat structures, which is actually achieved at relatively low aspect ratios of ~ 2 , the horizontal dipolar (quadrupolar) impedance equals half (minus half) the value of the transverse impedance of an axially symmetric structure with the same vertical profile variation. For the vertical impedance the scaling $Z_{Dy} \propto w$ predicted in [3]

is observed for $w_{av}^2/\ell^2 \ll 1$, while for wider tapers vertical impedance saturates. Furthermore, GdfidL simulations indicate that as the structure gets flatter most of the growth in Z_{Dy} is due to long range wake, while the vertical kick factor saturates at about twice the value for the corresponding axially symmetric structure.

Finally, while our analytical approach assumes confocal variation of elliptical cross-section $a^2 - b^2 = const$, GdfidL results for all impedances are rather insensitive to horizontal variations. Therefore our results could approximate a case of arbitrary ellipse variation with z , by considering a confocal structure with $b(z)$ matched everywhere and $a(z)$ matched at its minimum.

REFERENCES

- [1] K. Yokoya, CERN SL/90-88 (AP), 1990.
- [2] G.V. Stupakov, PAC-2001, p.1859. and SLAC-PUB-7086, 1995.
- [3] G.V. Stupakov, SLAC-PUB-7167, 1996.
- [4] B. Podobedov, S. Krinsky, PAC-2005, p. 1535.
- [5] A. Chao, S. Heifets, B. Zotter, Phys. Rev. ST-AB **5**, 111001 (2002), (and references there).
- [6] K. Yokoya, Part. Accel. **41** (1993), p. 221.
- [7] B. Podobedov and S. Krinsky, Phys. Rev. ST-AB **9**, 054401, (2006).
- [8] W. Bruns, <http://www.GdfidL.de>.